Atomic layer etching of CAR/SOG in EUV patterning of 300 mm wafers – selectivity and roughness mechanisms

Future technological nodes (N3 and below) will see further shrinking of not only the pattern dimensions, but of photoresist film-thickness as well. The etching of Spin-On-Glass (SOG) using a Chemically-amplified-resist (CAR) mask following lithography is strongly affected by this trend as the selectivity of the conventional etch processes will soon no longer be sufficient. Furthermore, roughness reduction techniques as we know them will also be challenged as they typically consume some of the already-meagre CAR budget. Therefore, the reactive-ion-etching – based atomic layer etching (RIE-ALE) of SOG with a CAR mask is investigated as a softer and more selective alternative to conventional RIE.

The RIE-ALE of SOG and the transfer into underlying hard mask have been demonstrated on coupons as well as on 300 mm full wafers, highlighting a strong increase of selectivity compared to RIE in coupons (Figure 1). However, the ALE process also yielded a higher roughness than RIE which doesn't meet the requirements for EUV patterning.

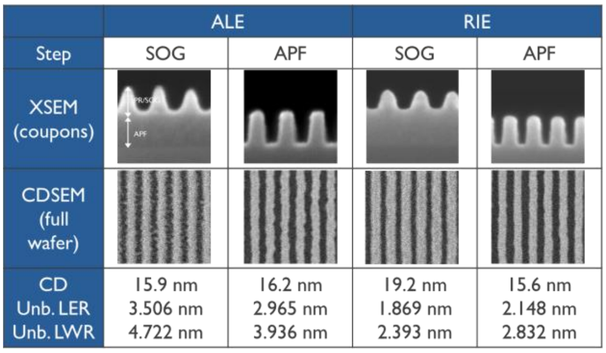

	ALE		RIE	
Step	SOG	APF	SOG	APF
XSEM (coupons)				
CDSEM (full wafer)				
CD	15.9 nm	16.2 nm	19.2 nm	15.6 nm
Unb. LER	3.506 nm	2.965 nm	1.869 nm	2.148 nm
Unb. LWR	4.722 nm	3.936 nm	2.393 nm	2.832 nm

Figure 1. XSEM (coupons) and CDSEM (full wafer) of the optimized ALE and RIE processes, the CD and unbiased LER & LWR are provided.

An investigation of the mechanisms leading to this improvement of selectivity together with the deterioration of the roughness is provided, highlighting the lack of chemical contrast due to the reactivity of the fluorocarbons, the role of redeposition mechanisms and the importance of interfacial interactions.

Indeed, the mechanisms of fluorination during the patterning process become essential to understand and optimize the processes, as the very thin layers become deeply modified within their bulk (Figure 2).

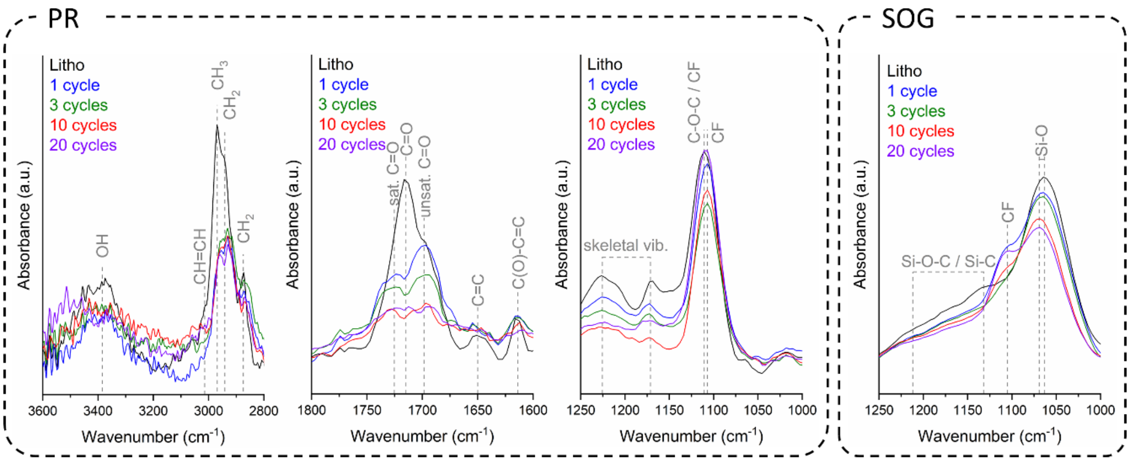

Figure 2. Chemical analyses of the fluorination of the PR and SOG layers by FTIR.

The selectivity observed on patterned wafers can be explained by redeposition mechanisms, as the fluorocarbon-mixed layers formed in ALE are sputtered and redeposit on the CAR mask (Figure 3).

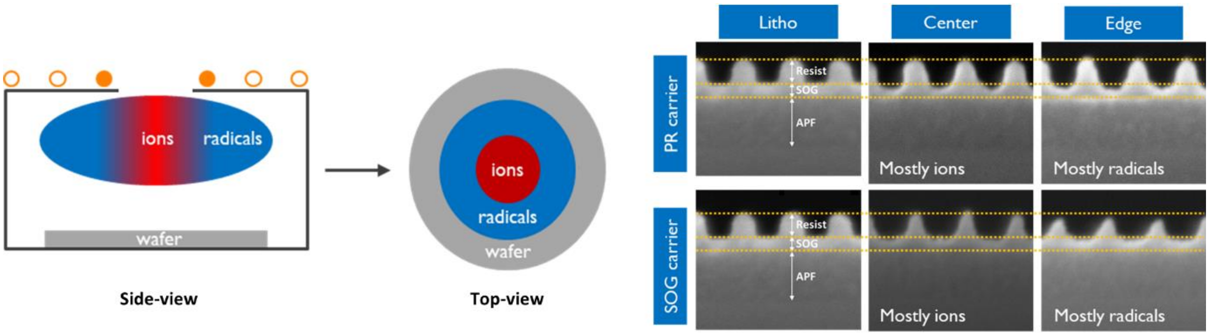

Figure 3. Spatial separation of the ions and radicals in the plasma with the ions being mostly in the center and the radicals being mostly on the edges. The effect on the selectivity by XSEM on coupons based on the loading is given.

Redeposition mechanisms are not suitable for an optimal roughness control as their statistical distribution leads to an increase of the LER and LWR. Moreover, the surface properties of both the CAR photoresist and SOG underlayer being deeply altered during the fluorination, the formation of complex interfaces as the ALE process occurs are expected to occur which induce further stress – hence roughness – within the layers. Surface free energy (SFE) measurements highlight the evolution of the dispersive $\Delta\gamma^{Disp}$ (*i.e.*, London force) and polar $\Delta\gamma^{Polar}$ (*i.e.*, Coulomb force) components of the layers during the patterning. Those interactions driving the gas to solid interactions before the formation of the mixed layer and the interface with the bulk, they provide valuable information on the potential stress within the stack (Figure 4).

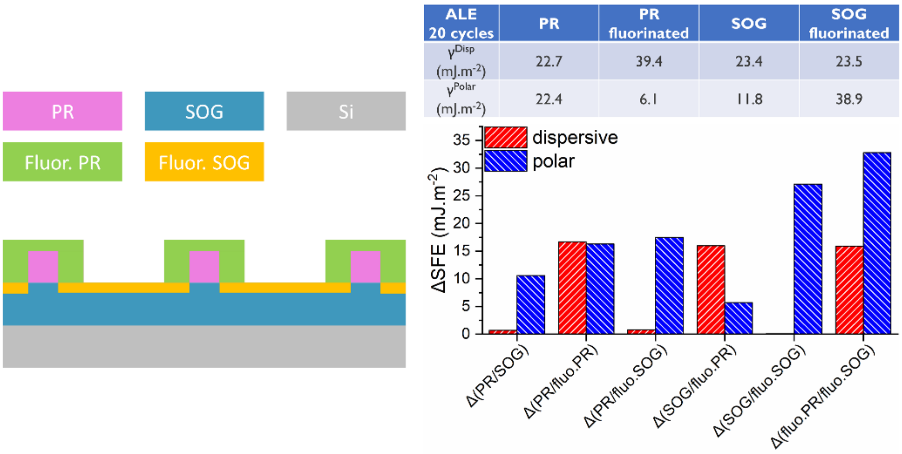

ALE 20 cycles	PR	PR fluorinated	SOG	SOG fluorinated
γ^{Disp} (mJ.m^{-2})	22.7	39.4	23.4	23.5
γ^{Polar} (mJ.m^{-2})	22.4	6.1	11.8	38.9

Figure 4. Scheme of the interface formation during the ALE process, the dispersive $\Delta\gamma^{Disp}$ and polar $\Delta\gamma^{Polar}$ component of the unaltered and fluorinated layers are provided. A qualitative comparison of the physical force mismatch for both forces is given.